

# PROPOSAL OF AN X-BAND LINEARIZER FOR DALIAN COHERENT LIGHT SOURCE

Guanglei Wang<sup>1</sup>, Qinming Li<sup>1</sup>, Weiqing Zhang<sup>1</sup>, Chao Feng<sup>2</sup>, Haixiao Deng<sup>2</sup>, Xueming Yang<sup>1</sup>

<sup>1</sup>State Key Laboratory of Molecular Reaction Dynamics, Dalian Institute of Chemical Physics, Chinese Academy of Sciences, Dalian 116023, P. R. China

<sup>2</sup>Shanghai Institute of Applied Physics, Chinese Academy of Sciences, Shanghai, 201800, P. R. China

## Abstract

Dalian coherent Light Source (DCLS) is a FEL user facility working at 50-150 nm, now under commissioning in Dalian, China. The facility based on HGHG mode, requires high brightness electron beam with small energy spread and low emittance. To compensate the nonlinearities in the e-beam longitudinal phase space, an X-band linearizer is considered before the bunch compressor. In this paper, we study the performance improvement of DCLS FEL radiation by using such a harmonic cavity, including the jitter of central wavelength induced by arriving time and a larger bunch compression ratio for femtosecond FEL application.

## INTRODUCTION

Seeded free-electron lasers (FELs) hold great promise for generating high brilliance radiation pulses with a narrow bandwidth. In order to satisfy the dramatically growing demands within the material, biological and chemical sciences, many FEL user facilities have been constructed and being proposed worldwide, from the extreme ultraviolet (EUV) to hard x-ray spectral region [1-5]. Dalian Coherent Light Source (DCLS) is a FEL user facility based on the principle of single-pass, high-gain harmonic generation [6], which is located in Dalian, China. With the state-of-the-art techniques of optical parametric amplification (OPA) seed laser and flexible gap undulator, DCLS is dedicated at EUV spectral regime of 150-50nm with pulse energy exceeds 100μJ.

DCLS will firstly focus on the physical chemistry with time-resolved pump-probe experiments and EUV absorption spectroscopy techniques. The time domain experiments are mainly related to the FEL pulse duration, e.g., less than 100fs, which can be easily achieved by utilizing an ultra-short seed pulse or emittance spoiler. However, another important and inevitable issue associated with both the time and spectral domain experiments for DCLS is FEL spectrum stability, i.e., shot-to-shot fluctuation, which will be strongly sensitive to numerous error sources of the electron beam and the seed laser time jitter. As we known, an electron bunch with relatively uniform energy distribution is crucial for the FEL performance and the beam energy curvature may degrade the output radiation pulse quality of seeded FELs, harmonic cavity is a universal method for compensating the energy chirp accumulated in the acceleration process. The DCLS e-beam and FEL pulse energy stabilities has been comprehensive studied in [6]. In this paper, we take a comparison

of DCLS radiation performance with and without X-band linearizer in LINAC [7], the results of spectrum stabilities is summarized in Section 3. In section 4, we concentrate on the advantage of X-band linearizer in fs FEL generation, a 2 times larger bunch compression ratio is introduced to the e-beam, the FEL peak power is improved about 4 times and the FEL spectrum is also better in X-band case.

## DCLS LAYOUT AND MAIN PARAMETERS

DCLS is designed as a fully coherent FEL user facility, which wavelength can be continuously tuned from 50 nm to 150 nm. The layout of DCLS (seen in Fig.1) consists of linear accelerator, undulator system and a seed laser system. In the nominal design of DCLS, an 300 MeV electron beam with sliced energy spread of 30 keV, e.g., a relative energy spread of  $1 \times 10^{-4}$ , normalized emittance better than 1.0 μm-rad, bunch charge of 500 pC, and peak current of 300 A is expected at the exit of the LINAC for efficient FEL lasing. The undulator system includes 1 segment of modulator and 6 segments of radiator, where the period length is 50mm and 30mm, respectively. What's more, tapered undulator technique will also be utilized to further enhance the pulse energy to hundreds of micro-joule level [8-9]. Benefit from the OPA technique, the seed laser is tunable at the wavelength range of 240-360nm, the seed laser pulse energy is more than 100μJ, and the pulse duration can be switched between 1ps and 100fs, thus to generate FEL pulse with different temporal properties.

As we known, an electron bunch with relatively uniform energy distribution is very important for FEL performance. Harmonic cavity is a universal method for compensating the energy chirp accumulated in the acceleration process. When a beam passing through two rf structures with wave number at  $k_{1,2}$ , peak energy gains  $E_{1,2}$  and phase  $\Phi_{1,2}$ , the energy of a particle at longitudinal position  $z$  with respect to the reference particle can be written as Eq.(1),

$$E(z) = E_1 \cos(\Phi_1 + k_1 z) + E_2 \cos(\Phi_2 + k_2 z), \quad (1)$$

the energy chirp will be canceled up to the second order when  $E_1 k_1^2 = E_2 k_2^2$ , the optimized voltage for the harmonic cavity scales as  $1/n^2$ , where  $n = k_2/k_1$  is the ratio of the two different wave number. Due to the contrary phase of the two different rf structures, the beam energy will also be unavoidable reduced by  $1/n^2$ .

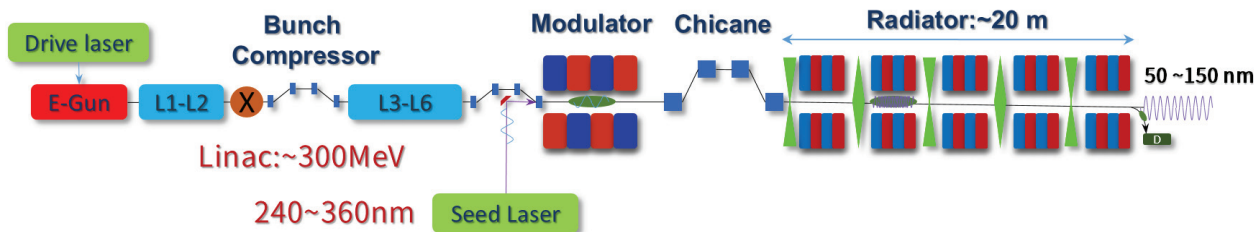


Figure 1: Schematic layout of DCL at HHG mode.

To estimate the e-beam performance improvement with an X-band linearizer, extensive simulations were performed in which various electron beam quantities and the seed laser timing were varied independently around their optimized values. In the simulation process, the electron beam dynamics in photo-injector was simulated with ASTRA [10] to take into accounts space-charge effects and ELEGENT [11] was used for the simulation in the remainder of the linac, the universal FEL simulating code GENESIS [12] was utilized to calculate the FEL performances, the beam energy and current distribution at the exit of the LINAC are summarized in Figure 2. Due to the e-beam chirp linearizer, a flatter electron beam energy can be achieved with X-band harmonic cavity, the position of the peak current is also located at the central part of the bunch.

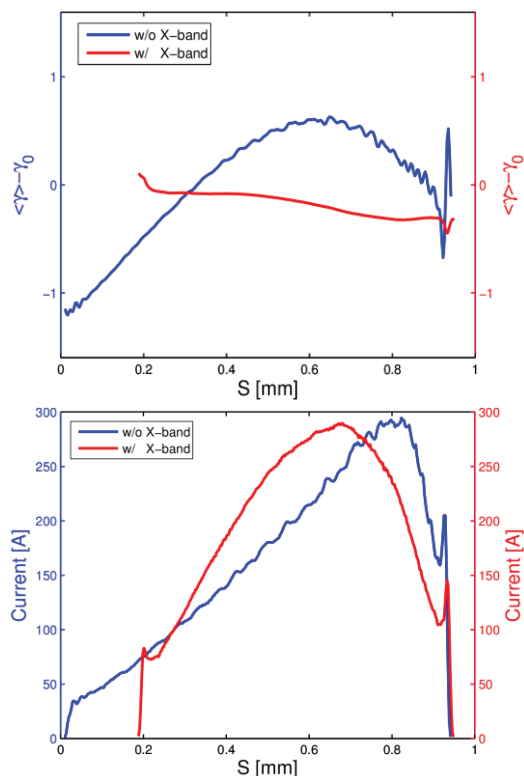


Figure 2: Beam energy and current distribution along the electron beam, with (red line) and without (blue line) X-band linearizer.

### EFFECT OF TIMING JITTER

For user operation, stability of central wavelength and the output pulse energy should be as good as possible, the jitter of FEL machine will definitely degrade the FEL performance. The e-beam sensitivity of LINAC is investigated by summing the uncorrelated random effects of DCLS, there is 250fs injector timing jitter, 5% bunch charge jitter, 0.1% RF voltage jitter,  $0.1^\circ$ RF phase jitter and 0.02% bunch compressor dispersion jitter, which leads a 0.09% beam energy jitter, 5.33% peak current jitter and 140fs beam arrival time jitter for current LINAC design. In this section, we concentrate on the effects of beam arriving time, the seed laser time jitter can be controlled smaller than 100 fs in DCLS.

Thus, we introduce a 200fs RMS timing jitter between the seed laser and e-beam, and focus on the spectrum stabilities in this section. Using the LINAC tracking results in Figure 2, start-to-end simulations were carried out. Here we show the details about the FEL operation. DCLS expects to generate 100 nm FEL radiation from the 300 nm seed laser with longitudinal Gaussian profile, 5 MW peak power. The FWHM length of the seed laser pulse is about 100 fs which is much shorter than the designed electron bunch length. Only a fraction of the beam is modulated in the modulator and produce coherent radiation in radiator. The moderate energy modulation amplitude is  $A_1 = 3$  in view of the tradeoff between the seed laser induced energy spread and the available bunching factor [13].

In the simulation, 100 shots were imported independently for FEL spectrum statistics, the seed laser modulates the e-beam randomly in the range of 200fs (RMS) around the optimal point. The results are summarized in Figure 3, the central wavelength shift in HHG is proportional to the energy chirp [14] and the laser pulse will interact with different part of electron beam with different energy chirp because of the timing jitter, the 100 nm FEL spectrum shows an obvious instability in the without X-band case, the standard derivation is about 0.2% of the 100nm wavelength. Utilizing the X-band linearizer, the e-beam energy is almost flat distribution in the optimized position, so a much stable wavelength output can be achieved. What's more, a direct seeding scheme is also proposed as an alternative options in DCLS, direct-seeding scheme will amplify the initial High Harmonic Generation (HHG) signal, so there is no influence of energy chirp in output spectrum (blue curve

in Figure 3). The spectrum of direct-seeding is narrower than HGHG, this is because the noise degradation in HGHG is proportional to the harmonic number  $n$  and a much more serious noise amplification happened in the harmonic conversion process [15].

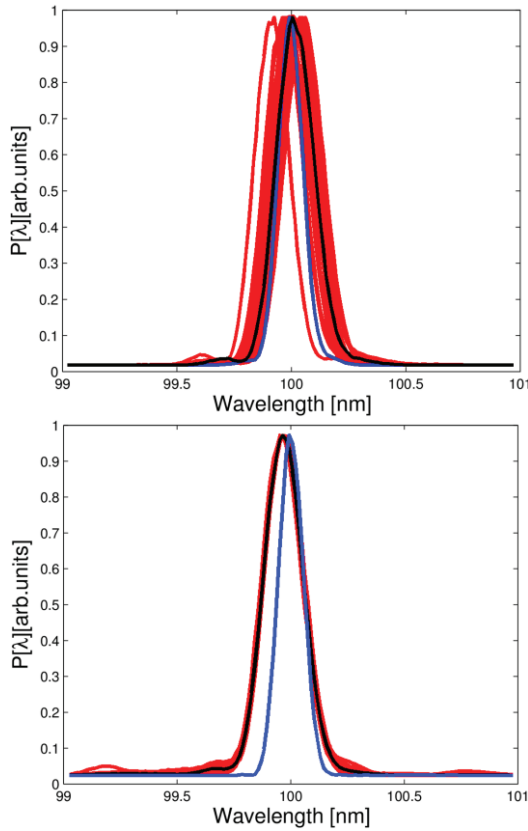


Figure 3: The HGHG spectrum of 100nm at saturation with time jitter (red line) and without time jitter (black line), direct-seeding spectrum (blue line). X band disabled (left) and X band enabled (right).

Finally, when the seed laser pulse length is comparable with the e-beam, the tolerance requirement on timing between the electron beam and the seed laser will be much relaxed, the wavelength jitter will also be better.

### X-BAND LINEARIZER IN FS FEL GENERATION

The nominal bunch length is 2 ps (FWHM) in DLCS, when the FEL is operated in 100fs level, most of the e-beam is unused. In order to increase the efficiency of FEL process, the e-beam is further compressed to 700 A and the beam energy and current distribution is shown in Figure 4.

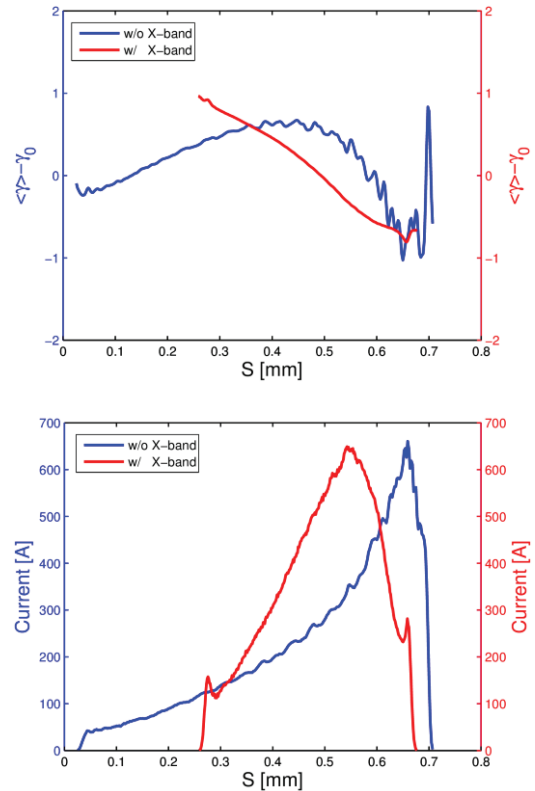


Figure 4: Beam energy and current distribution along the electron beam, with (red line) and without (blue line) X-band linearizer.

As mentioned in 1D theory, the FEL radiation power can be estimated with  $P_{FEL} = \rho P_{ebeam}$  [16],

$$\rho = \frac{1}{4\gamma} \left[ \frac{I}{I_A} \frac{\lambda_u^2 K^2 [JJ]^2}{\pi^2 \epsilon_x \beta_x} \right]^{1/3}$$

is the Pierce parameter of FEL, where  $\gamma$  is the beam energy,  $\lambda_u$  is the period length of undulator,  $K = 0.934 \cdot \lambda_u(cm) \cdot B(T)$  is the dimensionless undulator parameter,  $[JJ] = J_0\left(\frac{K^2}{4+2K^2}\right) - J_1\left(\frac{K^2}{4+2K^2}\right)$  is the modified Bessel function,  $I_A = 17kA$  and  $\epsilon_x$  is Alfvén current and normalized emittance, respectively. According to the 1D theory, the increase of e-beam peak current will lead to the increase of FEL radiation power and shorten the gain length in FEL process.

Figure 5 shows the simulation results of FEL peak power evolution along the undulator coordinate, FEL parameters are mentioned above and we use the same optimization methods to achieve the largest pulse energy in the simulation. Two times increase in the peak current, lead to about 2 times increase of FEL radiation pulse energy without X-band linearizer. When the X-band in, 4 times energy increase can be observed. What's more, the saturation length of 700A case is also shorter than the 300A, which are 5 m and 6 m, separately. At the exit of the undulator, FEL pulse energy of the two case is tending towards to identical, this is due to the unavoidable increase of the SASE radiation of the whole e-beam. For the comparison of spectra, After passing through 5 m long radiator, the relative FWEHM bandwidth of the dashed red line (w/ X-band ~300A) is about 0.12%, the noisy

spike and FEL spectrum broaden in the other cases are induced mainly by the nonlinear energy chirp in the electron beam [17–20]. Different methods for the generation of femtosecond FEL are also considered for DCLS, including the emittance spoiler, direct-seeding and so on [21,22], which are beyond the scope of this article.

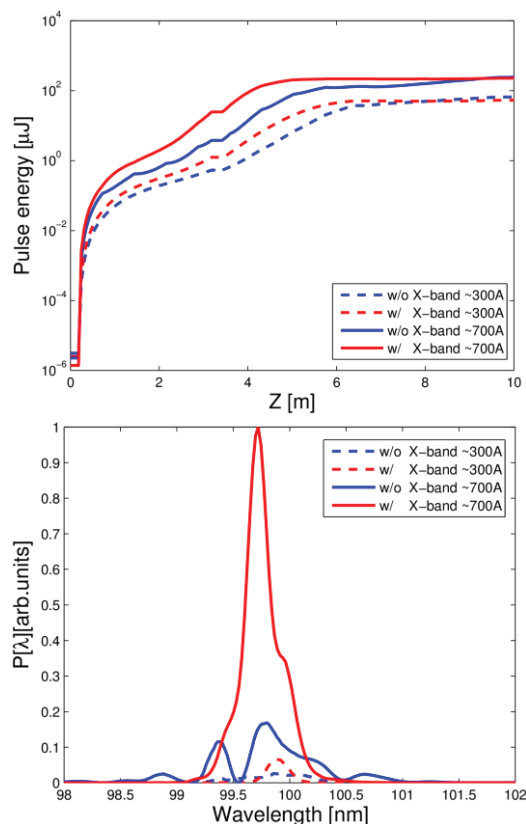


Figure 5: Comparison of final 100 nm radiation pulse energy (a) and spectra (b) of DCLS with a single-stage HGHG, the spectra are exported at the point of FEL bunching saturation, the red solid line (w/ X-band ~700A), the blue solid line (w/o X-band ~700A), the red dashed line (w/ X-band ~300A), the blue dashed line (w/o X-band ~300A).

### CONCLUSION

Dalian Coherent Light Source is expected to generate fully coherent laser pulses by seeded FEL scheme in the wavelength range between 150–50 nm with pulse photon number of  $10^{13}$  order. In this paper, with the help of intensive start-to-end FEL simulations, performance improvement of an X-band linearizer is investigated. A much more stable output wavelength can be achieved

with X-band. In fs FEL generation, larger compression ratio can be realized in X-band case and results in a 4 times increase of FEL power with current DCLS layout. The X-band linearizer will provide an e-beam with better distribution of emittance, energy spread and beam current, results in a more pure radiation spectrum for DCLS. The application of X-band system can play an importance role for the DCLS performance improvement.

### ACKNOWLEDGEMENT

The authors are grateful to Bo Liu and Meng Zhang for helpful discussions. This work was supported by the National Natural Science Foundation of China (21127902, 11175240, 11205234 and 11322550).

### REFERENCE

- [1] McNeil B., Thompson N., *Nature Photon*, 2010, 4: 814
- [2] Ackermann W *et al.*, *Nature Photon*, 2007, 1: 336
- [3] Emma P *et al.*, *Nature Photon*, 2010, 4: 641
- [4] Ishikawa T *et al.*, *Nature Photon*, 2012, 6: 540
- [5] Allaria E *et al.*, *Nature Photo*, 2012, 6: 699
- [6] Haixiao Deng *et al.*, *Chin. Phys. C*, 2014 38: 028101
- [7] Linac Coherent Light Source Conceptual Design Report No. SLAC-R-593, 2002.
- [8] Wang, X. J. *et al.*, *Phys. Rev. Lett.*, 2009, 103, 154801.
- [9] Mak, A *et al.*, *Phys. Rev. ST Accel. Beams.*, 2015, 18, 040702
- [10] K. Floettmann, *ASTRA User's Manual*, Available at: [http://www.desy.de/mpyf10/Astra\\_dokumentations](http://www.desy.de/mpyf10/Astra_dokumentations)
- [11] M. Borland, Advanced Photon Source LS 287(2000).
- [12] S. Reiche, *Nucl. Instr. and Meth. A*, 1999, 429, 243.
- [13] K. J. Kim, Z. R. Huang, R. Lindberg, Introduction to the physics of Free Electron Laser.
- [14] G.L. Wang *et al.*, *Nucl. Instrum. Methods A*, 737 (2014) 237.
- [15] E. L. Saldin *et al.*, *Optics Communications*, 202 (2002) 169.
- [16] P. Schmüser, M. Dohlus, J. Rossbach, Ultraviolet and Soft X-Ray Free-Electron Lasers.
- [17] E. L. Saldin, E. A. Schneidmiller, and M. V. Yurkov, *Opt. Commun.*, 202, 169 (2002).
- [18] D. Ratner *et al.*, *Phys. Rev. ST Accel. Beams*, 15, 030702 (2012).
- [19] C. Feng *et al.*, *Phys. Rev. ST Accel. Beams*, 16, 060705 (2013).
- [20] G. Wang *et al.*, *Nucl. Instrum. Methods Phys. Res., Sect. A* 753, 56 (2014).
- [21] P.Emma *et al.*, The Emittance Spoiler Foil: A Simple Method to Produce Femtosecond and Sub-Femtosecond X-Ray Pulses from a SASEBased Free-Electron Laser.
- [22] G. Lambert *et al.*, *Nature Physics*, Vol. 4 (2008) 296.